Island reduction using boundary perturbations.

NCSX Project Meeting
Sep 26-27 2000

S.R.Hudson, D.A.Monticello, M.Zarnstorff, A.H.Boozer

Abstract

- Islands are modeled using the PIES code. VMEC is used to prepare input files for PIES.
- The effect of making small changes the boundary on island size is investigated.
- By measuring the resonant fields at rational surfaces, partial derivatives relating small changes in the boundary to changes in resonant fields are calculated.
- This information is used to determine the boundary changes which will reduce the resonant fields and thus reduce island width. The configuration li383 is examined.

Outline

- Calculation of resonant fields — Quadratic-Flux Minimizing Surfaces
- Coupling Matrix — SVD analysis
- Example — li383 island reduction
- Pressure Induced Self Healing
- More Examples
- Future Work
- References

Quadratic Flux Minimizing Surfaces [1, 2]

- Resonant normal magnetic fields are responsible for islands. They may be calculated via the construction of quadratic-flux minimizing surfaces.
- The action integral is the integral of the magnetic vector potential $\mathbf{A}$ along a curve :

$$S = \oint \mathbf{A} \cdot \mathbf{dl} = \oint (A_\rho \dot{\rho} + A_\theta \dot{\theta} + A_\zeta) d\zeta, \tag{1}$$

- The quadratic-flux functional is a surface integral of the action gradient,

$$\varphi_2 = \frac{1}{2} \int \int \left[\frac{\delta S}{\delta \theta} \right]^2 d\theta d\zeta. \tag{2}$$

- An Euler-Lagrange equation is derived for extremal surfaces,

$$(B^\theta \partial_\theta + B^\zeta \partial_\zeta) \frac{\delta S}{\delta \theta} = 0, \tag{3}$$

- Quadratic-flux minimizing surfaces are comprised of a family of periodic pseudo field lines of the field tangential to the surface, along which the action gradient is constant.

$$\mathbf{B}_\nu \cdot \nabla \equiv (B^\theta \partial_\theta + B^\zeta \partial_\zeta) = \mathbf{B} - \nu \mathcal{J} \mathbf{e}_r \tag{4}$$

Quadratic-Flux Minimizing Surface – Example

Figure 1:

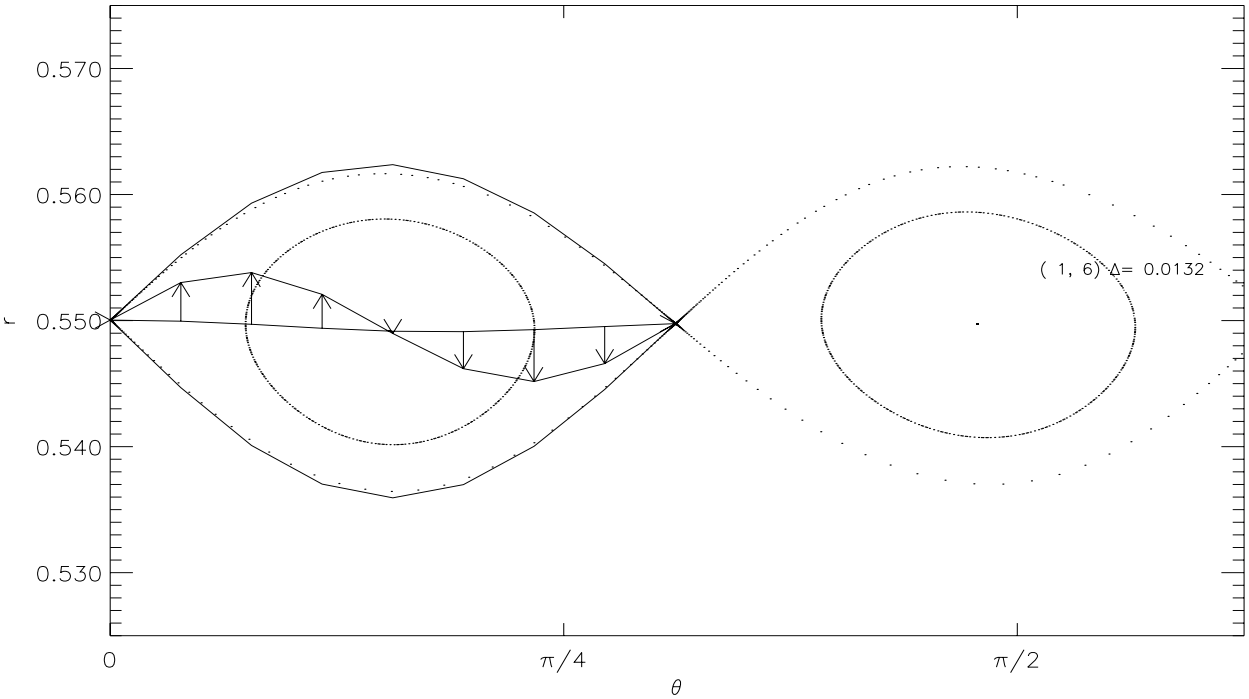

- The above plot shows the action gradient (normal field) with arrows. The quadratic-flux surface passes directly through the X and O points and is shown with a solid line. A Poincare plot with 3 starting points (at the X point, the O point and the mid point) is shown with dots.
- The construction of a quadratic-flux minimizing surface at a chosen island chain locates the X and O periodic trajectory, and entails a determination of the normal component of the magnetic field.
- If the shear of the 'underlying integrable field' is known, then island widths and separatrices may be precisely calculated. The separatrix is plotted with a solid line.
- Furthermore, quadratic-flux minimizing surfaces may be used to approximate KAM surfaces, and thus be used to partition regions of chaos, and provide a convenient set of surfaces for generalized magnetic coordinates for toroidal fields with islands and chaotic regions.

Coupling Matrix

- Variations $\delta B_{m,n}$ in resonant field amplitudes $B_{m,n}$ at rational ($\iota = 3m/n$) quadratic-flux-minimizing surfaces are related to variations in boundary harmonics $\delta_{n,m}$ via a coupling matrix C to which SVD method is applied

$$\boldsymbol{\delta}\mathbf{B}_{\mathbf{m,n}} = C\delta = UwV^T\boldsymbol{\delta} \tag{5}$$

- The coupling matrix is determined by adding a series of small harmonics (about one millimeter) to fixed boundary VMEC runs and running PIES (say for about 32 iterations).

- By choosing a perturbation $\boldsymbol{\delta}^R$ according to

$$\boldsymbol{\delta}^R = Vw^{-1}U^T\mathbf{B} \tag{6}$$

  where $\mathbf{B}$ are the original resonant fields, (and the singular values have been zeroed), a set of island reducing perturbations is obtained.

- If there are more variables than equations (ie. more boundary perturbations are considered than resonant fields), more than one solution exists (spanned by the null-space) and other physics properties of the configuration may be optimized.

- If fewer boundary perturbations than resonant fields are considered, one is satisfied with a best solution.

- The coupling matrix may be singular, indicating no solution for $\boldsymbol{\delta}^R$.

Example – li383 – rotational transform

- the rotational transform profile is used to identify rational surfaces present in a given configuration

Figure 2: full current full pressure li383 – rotational transform profile

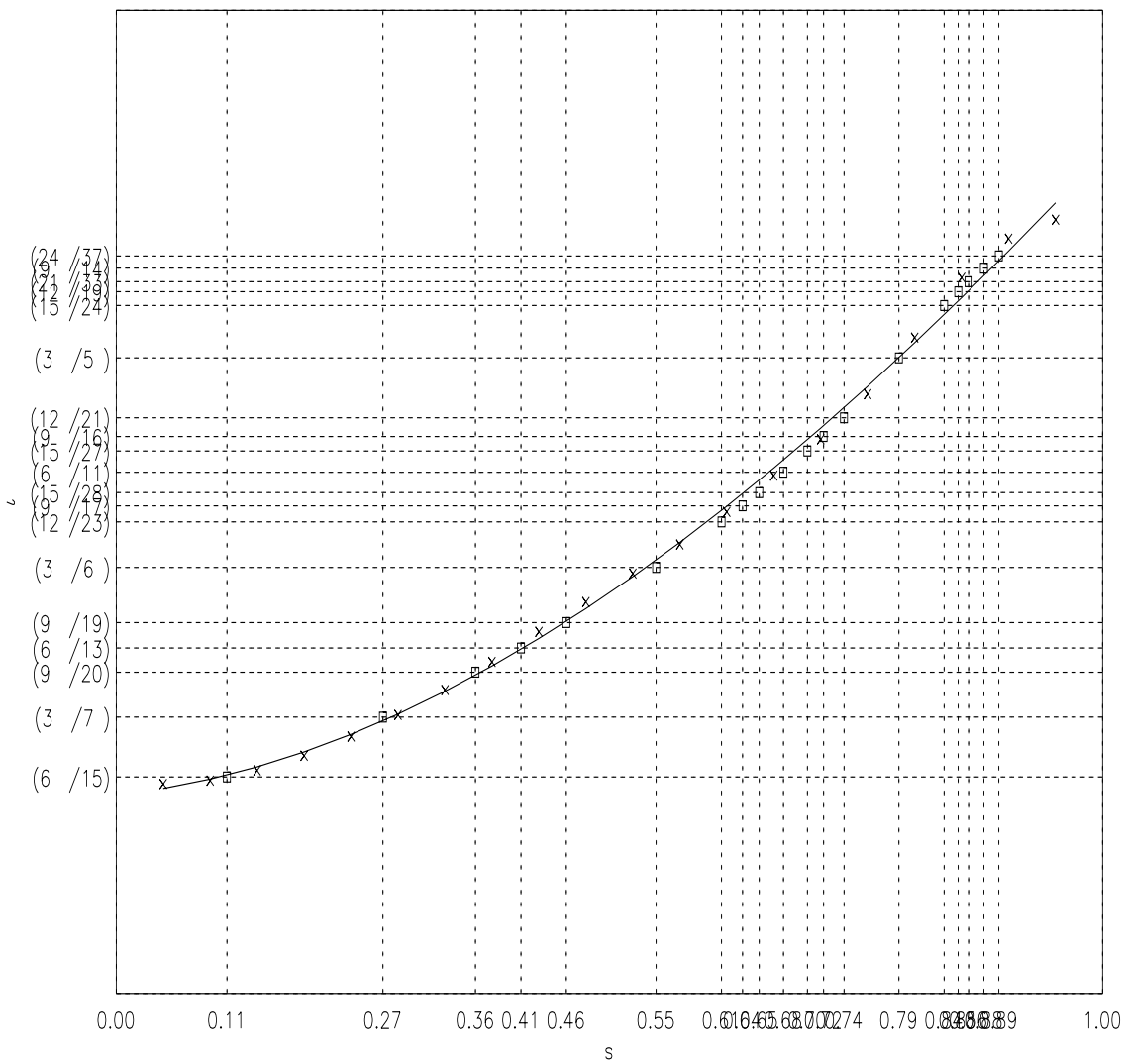

Example – li383 – initial configuration

Figure 3: full current full pressure li383 – Poincare plot

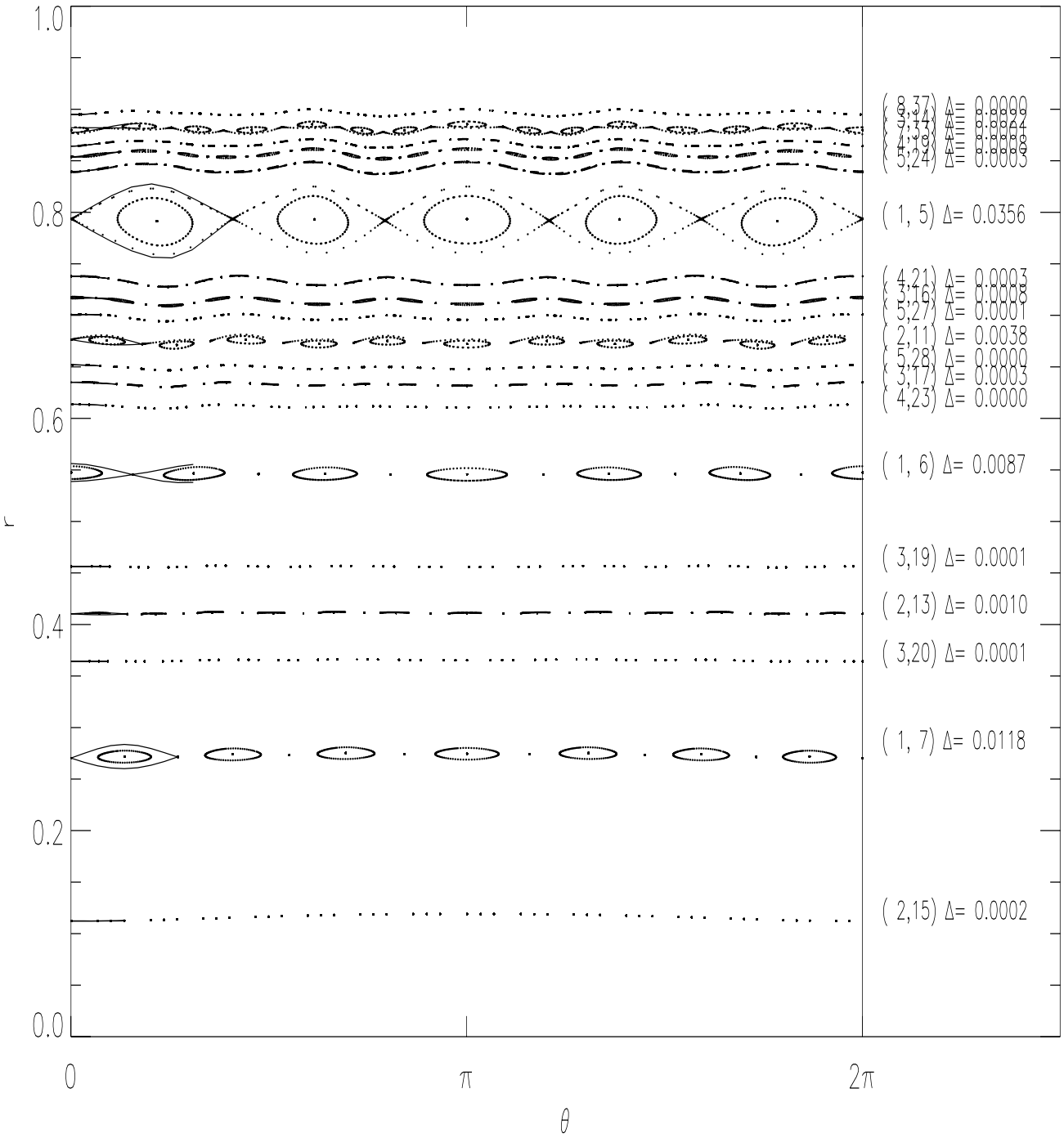

Example – li383 – coupling matrix

- A set of N boundary perturbations are chosen and N VMEC/PIES runs enables determination the coupling matrix :

$$\begin{pmatrix} \delta B_{1,7} \\ \delta B_{3,20} \\ \delta B_{2,13} \\ \delta B_{3,19} \\ \delta B_{1,6} \\ \delta B_{3,17} \\ \delta B_{2,11} \\ \delta B_{3,16} \\ \delta B_{1,5} \end{pmatrix} = \begin{pmatrix} -0.06124 & 0.03861 & -0.04465 & -0.08002 & -0.00859 \\ 0.00006 & -0.00025 & 0.00001 & 0.00003 & -0.00001 \\ -0.00756 & 0.00708 & -0.00029 & -0.00050 & -0.00057 \\ -0.00021 & 0.00056 & 0.00001 & 0.00012 & 0.00003 \\ -0.14365 & -0.44514 & 0.11457 & -0.30841 & -0.04901 \\ -0.00718 & 0.00486 & -0.00010 & 0.00183 & -0.00045 \\ -0.13048 & 0.00200 & -0.06524 & 0.02446 & 0.00307 \\ 0.02919 & -0.00438 & 0.00373 & -0.00278 & 0.00094 \\ 0.77286 & -0.74143 & -0.91646 & -0.15419 & -0.29131 \end{pmatrix} \begin{pmatrix} \delta_{1,8} \\ \delta_{1,7} \\ \delta_{1,6} \\ \delta_{1,5} \\ \delta_{1,4} \end{pmatrix} \quad (7)$$

$$\boldsymbol{\delta}^R = (\ -0.00002\ ,\ -0.00057\ ,\ 0.00161\ ,\ 0.00073\ ,\ 0.00211\ )^T \quad (8)$$

- With this perturbation, a new VMEC/PIES run is performed and the new resonant fields are measured :

initial	iter1		
0.00017	0.00008	$(1,7)$	47%
0.00000	0.00000		
0.00001	−0.00000		
0.00000	−0.00000		
−0.00011	0.00026	$(1,6)$	236%
0.00000	0.00000		
0.00008	−0.00009		
−0.00001	0.00000		
0.00180	−0.00003	$(1,5)$	2%

(9)

- The dominant $(1,5)$ harmonic is significantly reduced. The $(1,6)$ has doubled, but is still small.

li383 IR – results

Figure 4: li383-IR

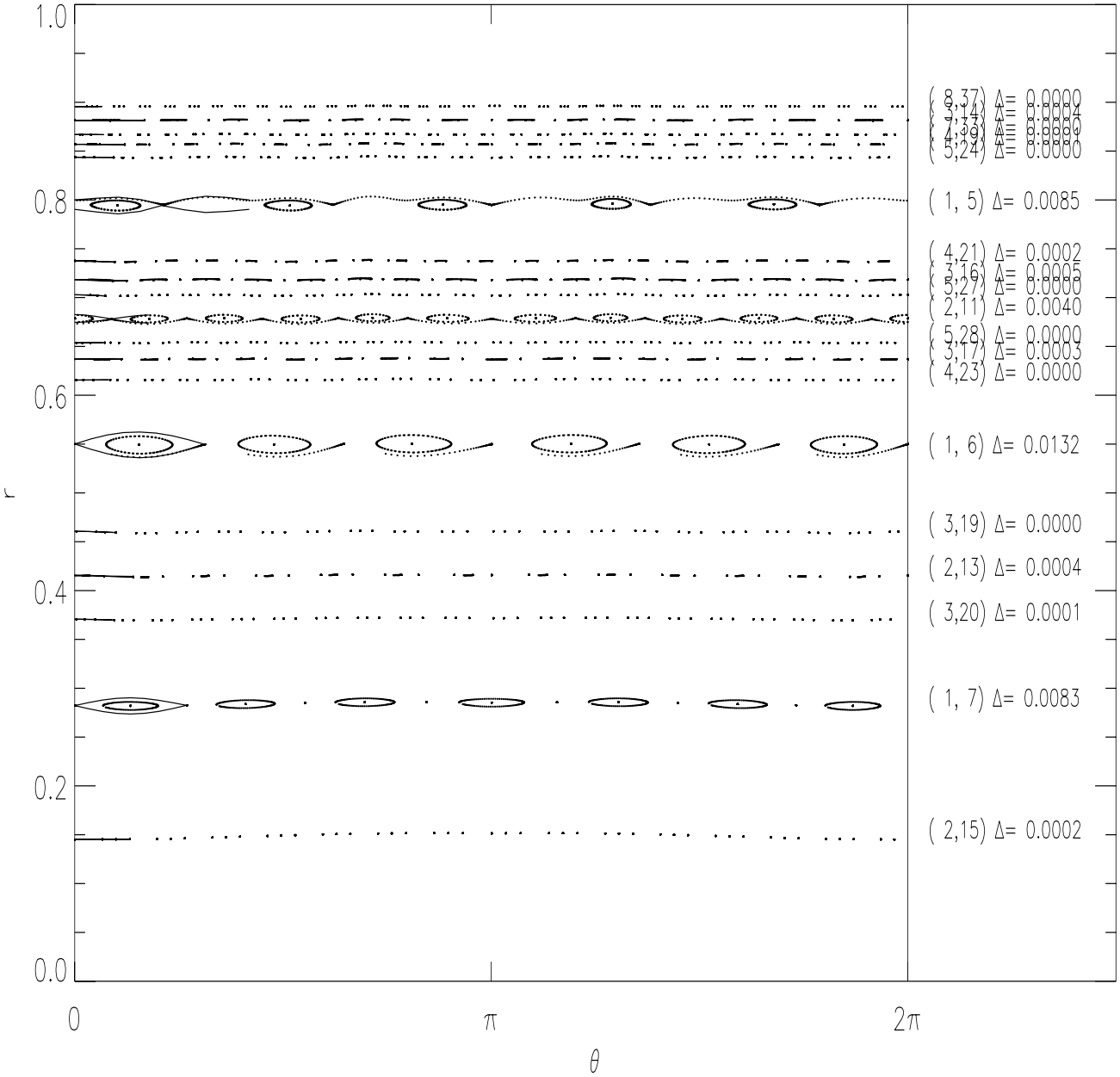

- the $(1, 5)$ island is reduced in size but a $(2, 10)$ (not targeted in present work) is now showing.

Pressure induced self-healing

- It was noted that the li383-IR configuration produced an increased $(1, 5)$ island as the pressure was lowered, suggesting pressure induced self-healing.

Figure 5: full current zero pressure li383-IR

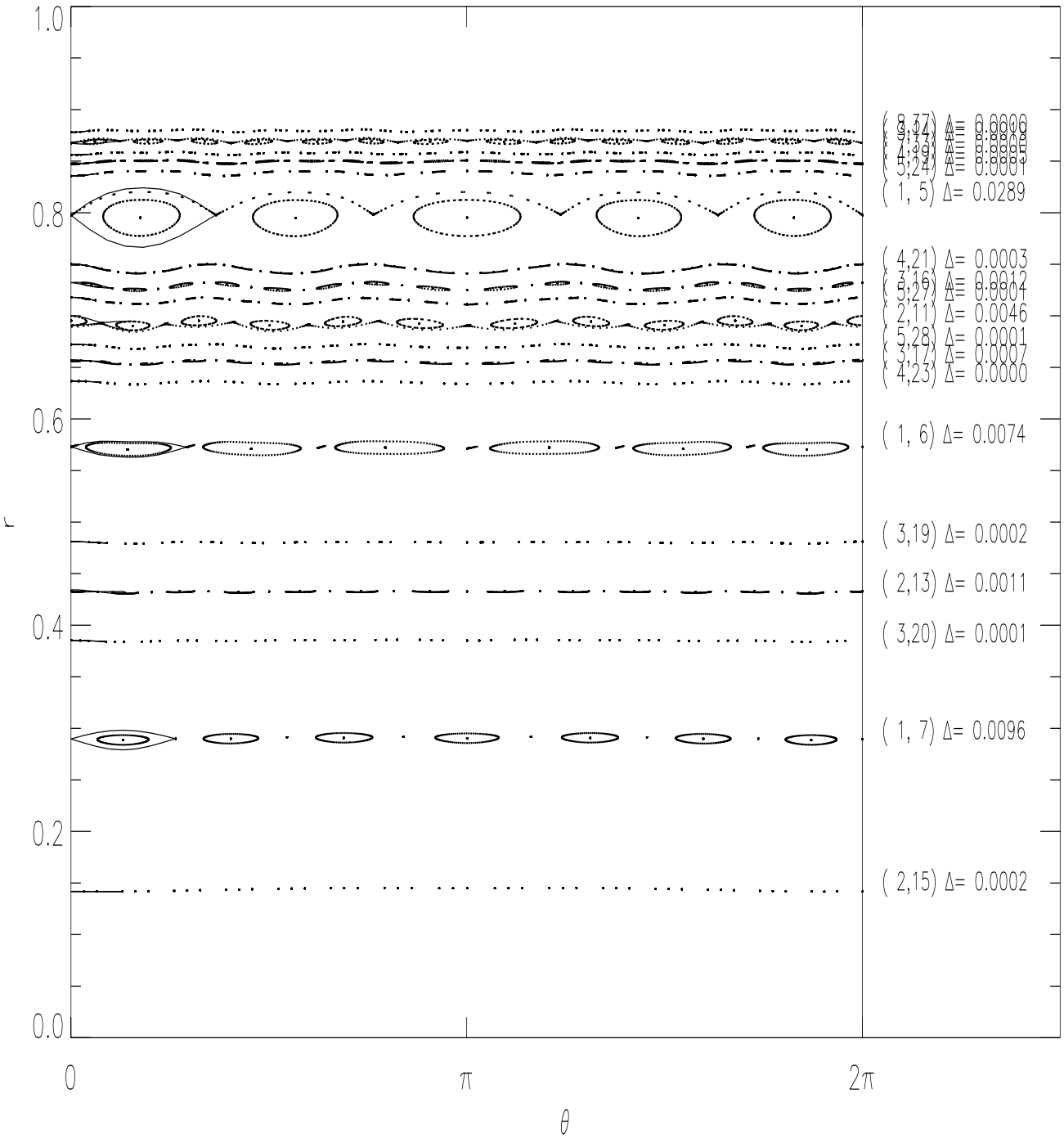

Example – li383 modular – case 1 – initial configuration

Figure 6: li383 modular – Poincare plot

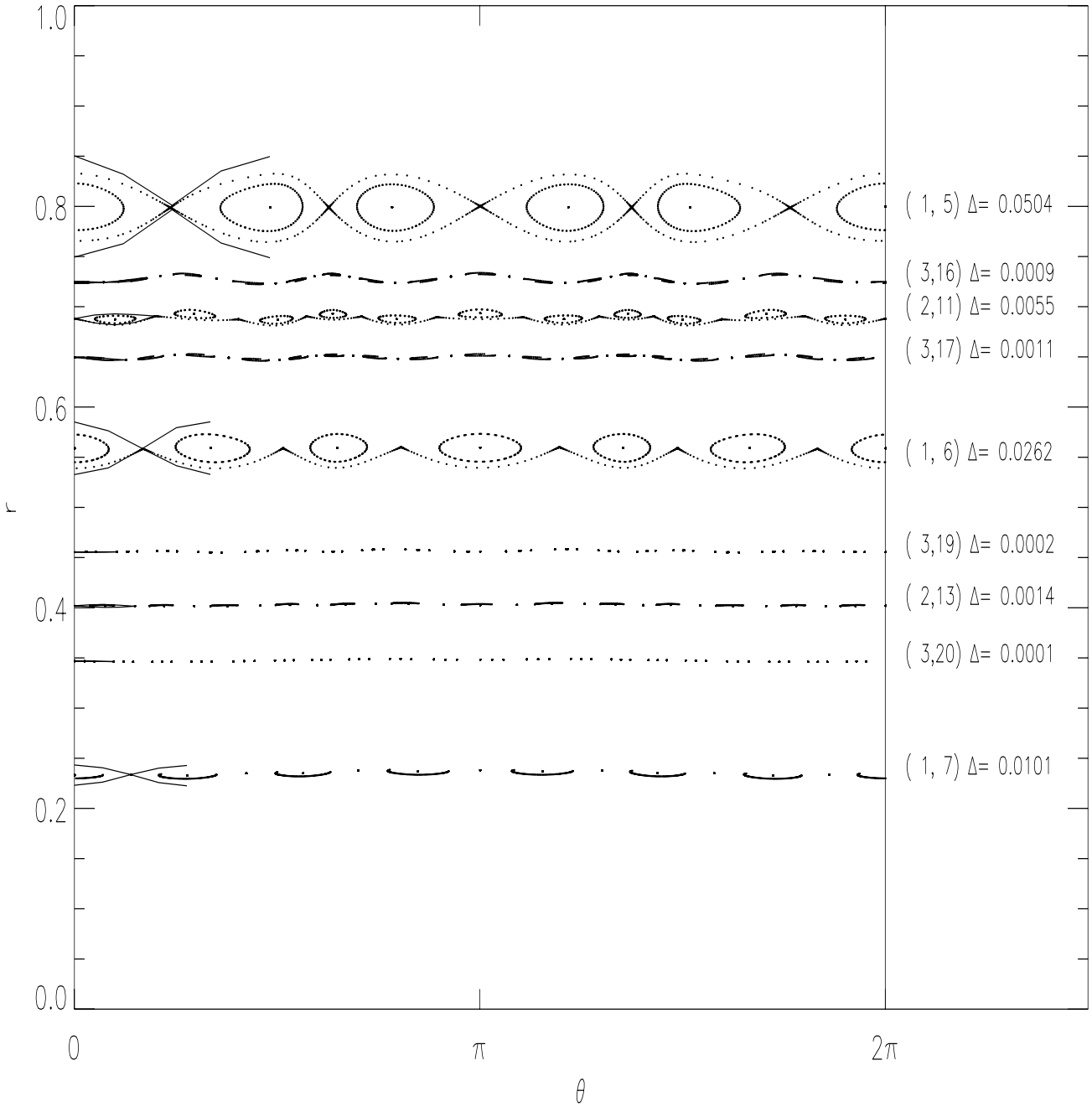

Example – li383 modular – case 1 – coupling matrix

$$\begin{pmatrix} \delta B_{1,7} \\ \delta B_{3,20} \\ \delta B_{2,13} \\ \delta B_{3,19} \\ \delta B_{1,6} \\ \delta B_{3,17} \\ \delta B_{2,11} \\ \delta B_{3,16} \\ \delta B_{1,5} \end{pmatrix} = \begin{pmatrix} -0.00745, & -0.01960, & -0.03878, & 0.11187, & 0.16382, \\ 0.00002, & 0.00006, & 0.00000, & 0.00000, & 0.00005, \\ 0.00432, & 0.01719, & -0.00421, & 0.00318, & -0.00065, \\ 0.00073, & 0.00266, & -0.00011, & 0.00053, & 0.00026, \\ -0.51694, & -1.64426, & 0.01973, & -0.62650, & 0.09014, \\ 0.00746, & 0.05556, & -0.00490, & 0.00524, & 0.00261, \\ 0.03254, & 0.38586, & -0.14787, & -0.00967, & -0.04361, \\ 0.00412, & 0.04030, & -0.02104, & -0.01292, & -0.00877, \\ 0.29009, & -1.06014, & -1.29179, & -0.52548, & -0.60014, \end{pmatrix} \begin{pmatrix} \delta_{1,8} \\ \delta_{1,7} \\ \delta_{1,6} \\ \delta_{1,5} \\ \delta_{1,4} \end{pmatrix} \quad (10)$$

$$\boldsymbol{\delta}^R = (\ 0.00529\ ,\ -0.00099\ ,\ -0.00078\ ,\ -0.00300\ ,\ 0.00257)^T \quad (11)$$

- With this perturbation, a new VMEC/PIES run is performed and the new resonant fields are measured.

initial	iter1	iter2	
−0.000096	0.000267	0.000087	(1, 7)
0.000000	−0.000001	0.000000	
0.000010	0.000032	0.000012	
0.000000	0.000002	0.000003	
−0.000981	0.000681	−0.000212	(1, 6)
0.000015	−0.000019	0.000008	
0.000175	0.000110	−0.000688	
−0.000011	0.000019	−0.000048	
−0.003621	−0.000713	−0.000213	(1, 5)

(12)

- The resonant fields decrease with iterations.

li383 modular IR – case 1 – after 1 iteration

Figure 7: li383-IR

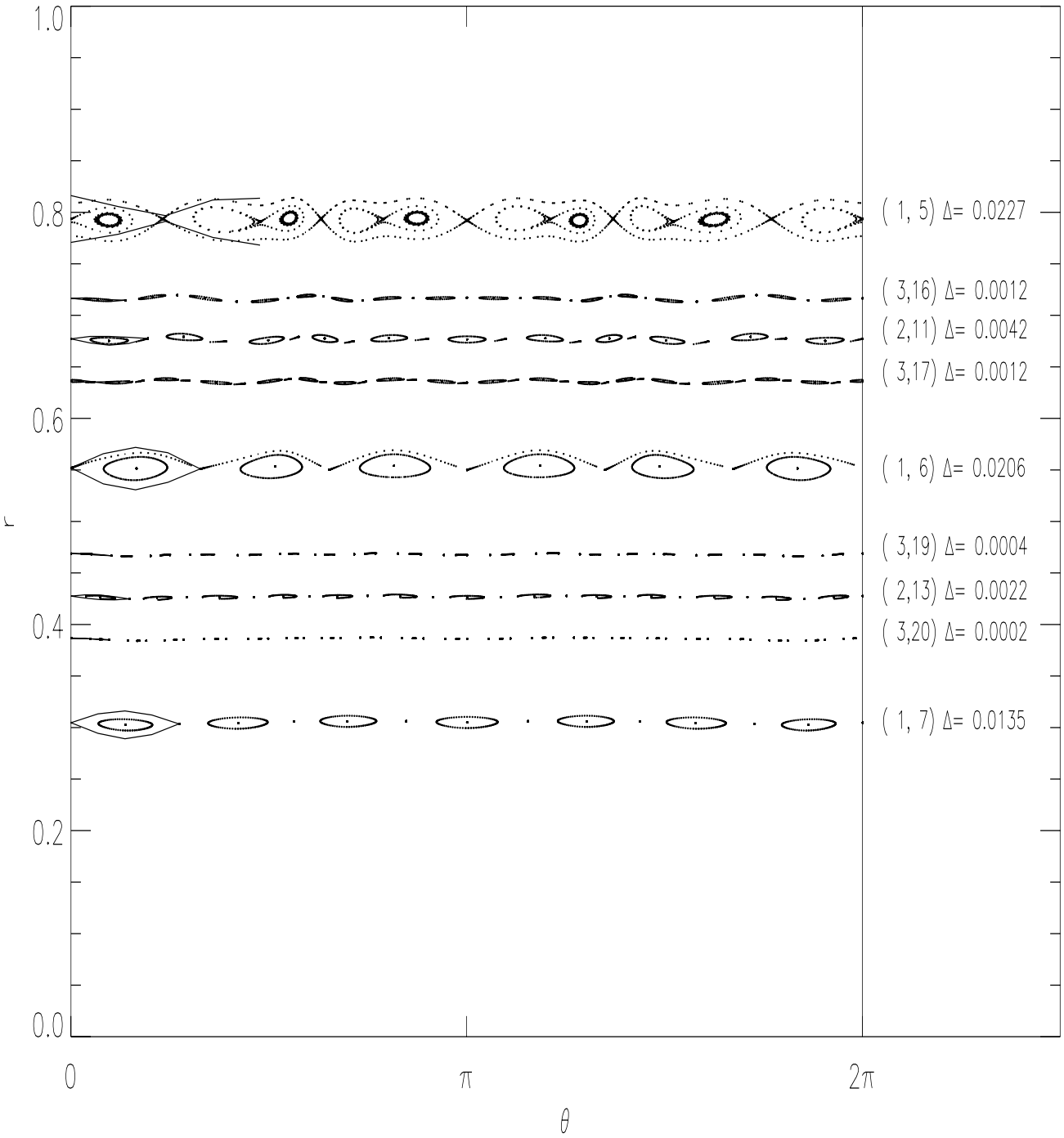

li383 modular IR – case 1 – after 2 iterations

Figure 8: li383-IR

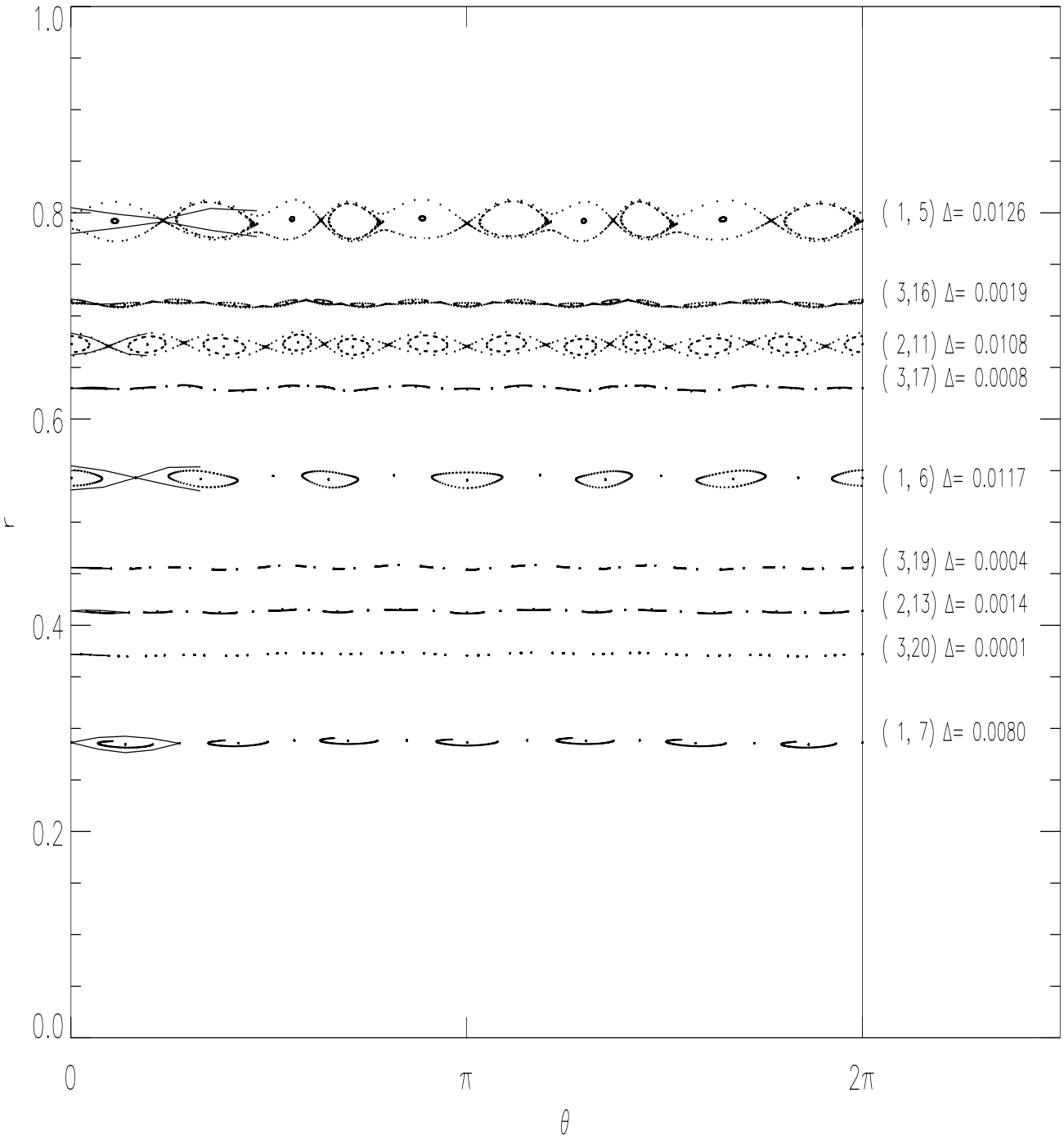

- The $(1,5)$ island is reduced in size but a $(2,10)$ (not targeted in present work) is now showing. The $(1,6)$ island is reduced.

Example – li383 modular – case 2 – initial configuration

Figure 9: li383 modular – Poincare plot

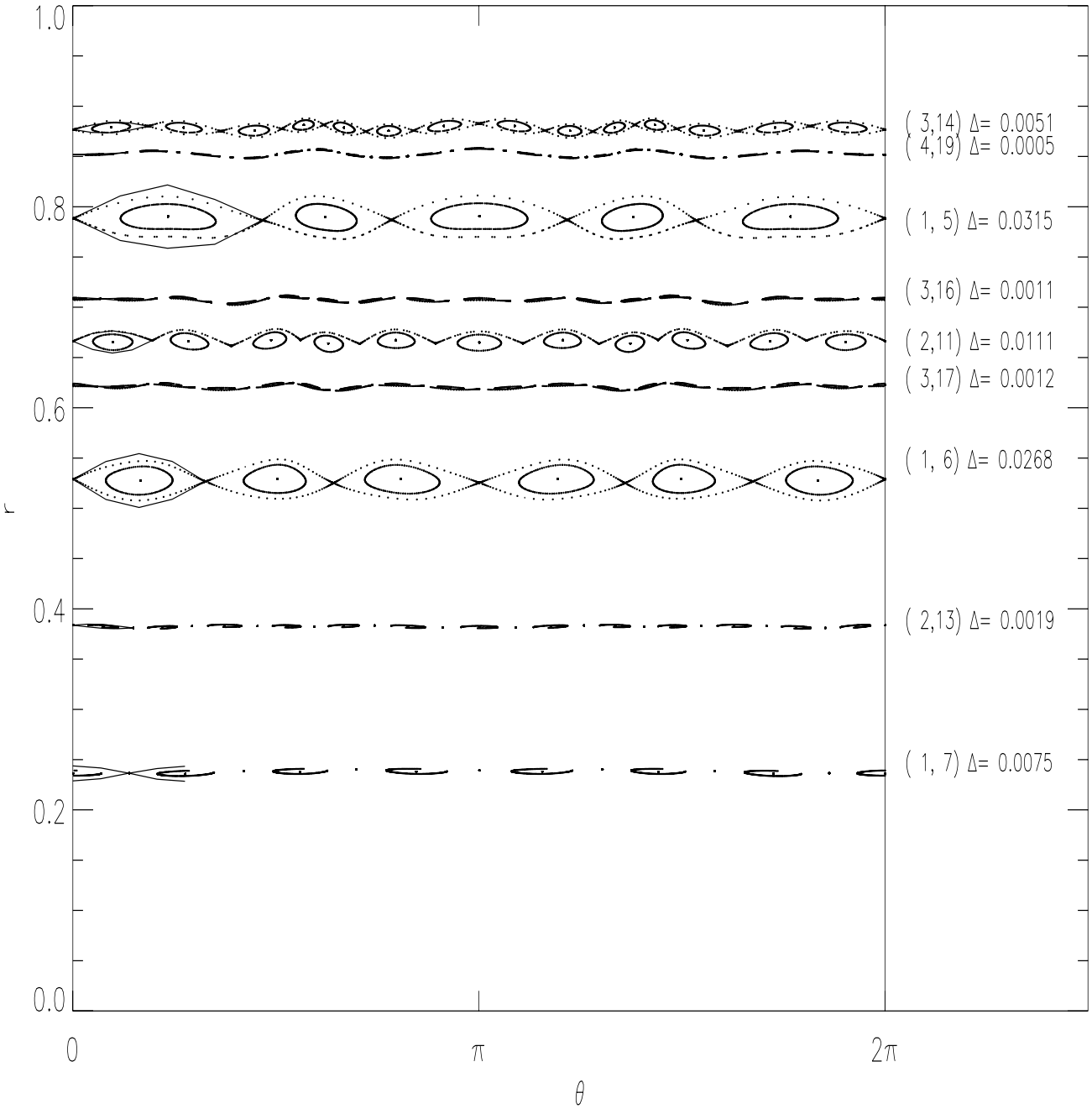

Example – li383 modular – case 2 – coupling matrix

$$\begin{pmatrix} \delta B_{1,6} \\ \delta B_{2,11} \\ \delta B_{1,5} \\ \delta B_{3,14} \end{pmatrix} = \begin{pmatrix} -0.67516, & -1.72788, & 0.24369, & -0.34000, & -0.48345, \\ -0.14784, & 1.37072, & 1.13847, & 1.34803, & -0.25746, \\ 0.15902, & -0.97402, & -1.09897, & -0.50774, & -0.71493, \\ -0.03325, & -0.05900, & -0.02396, & 0.06071, & -0.02650, \end{pmatrix} \begin{pmatrix} \delta_{1,8} \\ \delta_{1,7} \\ \delta_{1,6} \\ \delta_{1,5} \\ \delta_{1,4} \end{pmatrix} \quad (13)$$

$$\boldsymbol{\delta}^R = (\ 0.0007\ ,\ 0.0010\ ,\ 0.0015\ ,\ -0.0027\ ,\ 0.0002\ )^T \quad (14)$$

- With this perturbation, a new VMEC/PIES run is performed and the new resonant fields are measured :

initial	iter1	iter2	
0.001030	0.001443	0.000048	$\leftarrow (1,6)$
0.000697	0.000714	0.000683	$\leftarrow (2,11)$
0.001300	−0.000686	−0.000726	$\leftarrow (1,5)$
0.000291	0.000142	0.000185	$\leftarrow (3,14)$

(15)

li383 modular IR – case 2 – iteration 1

Figure 10: li383-IR

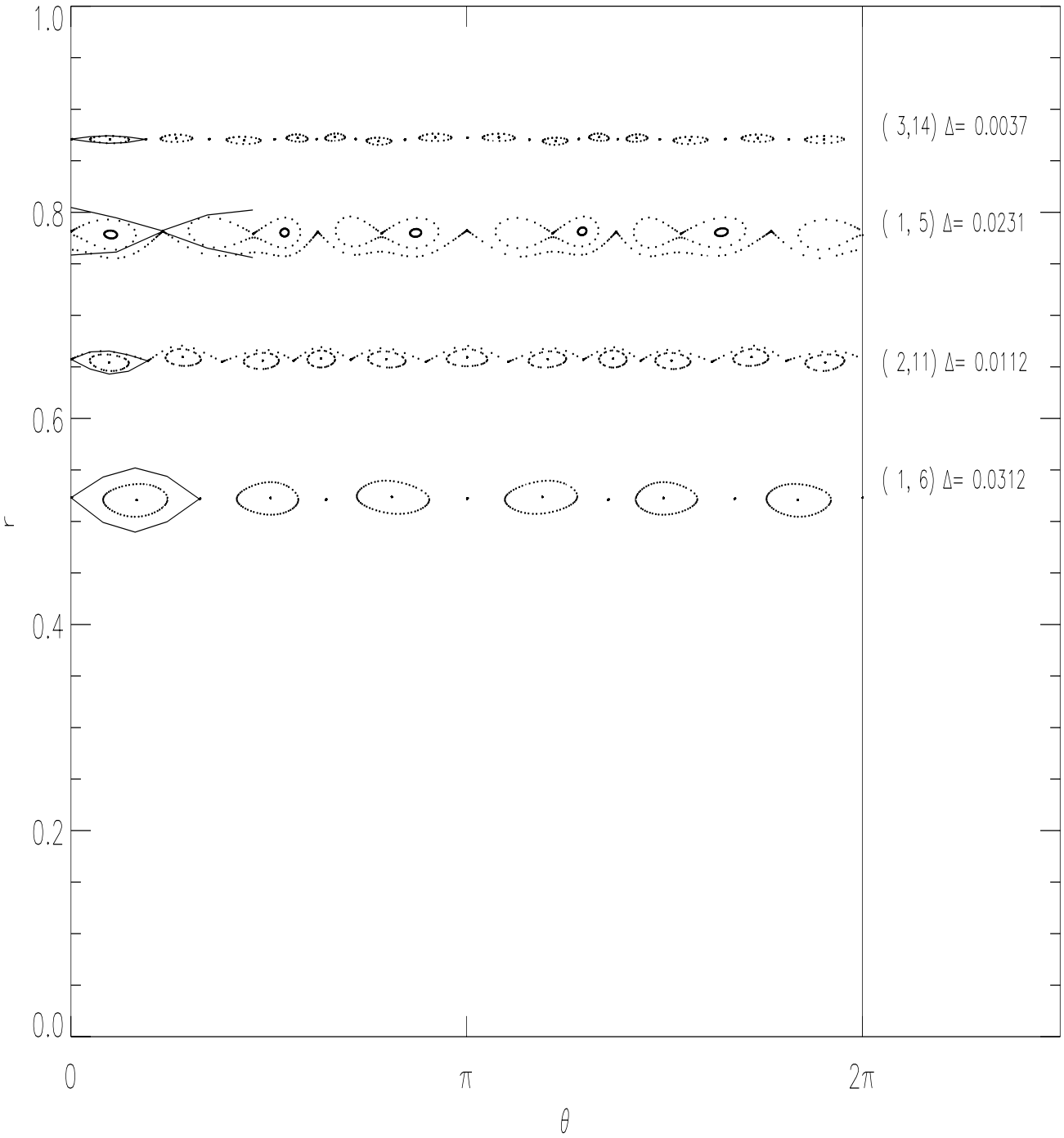

li383 modular iR – case 2 – iteration 2

Figure 11: li383-IR

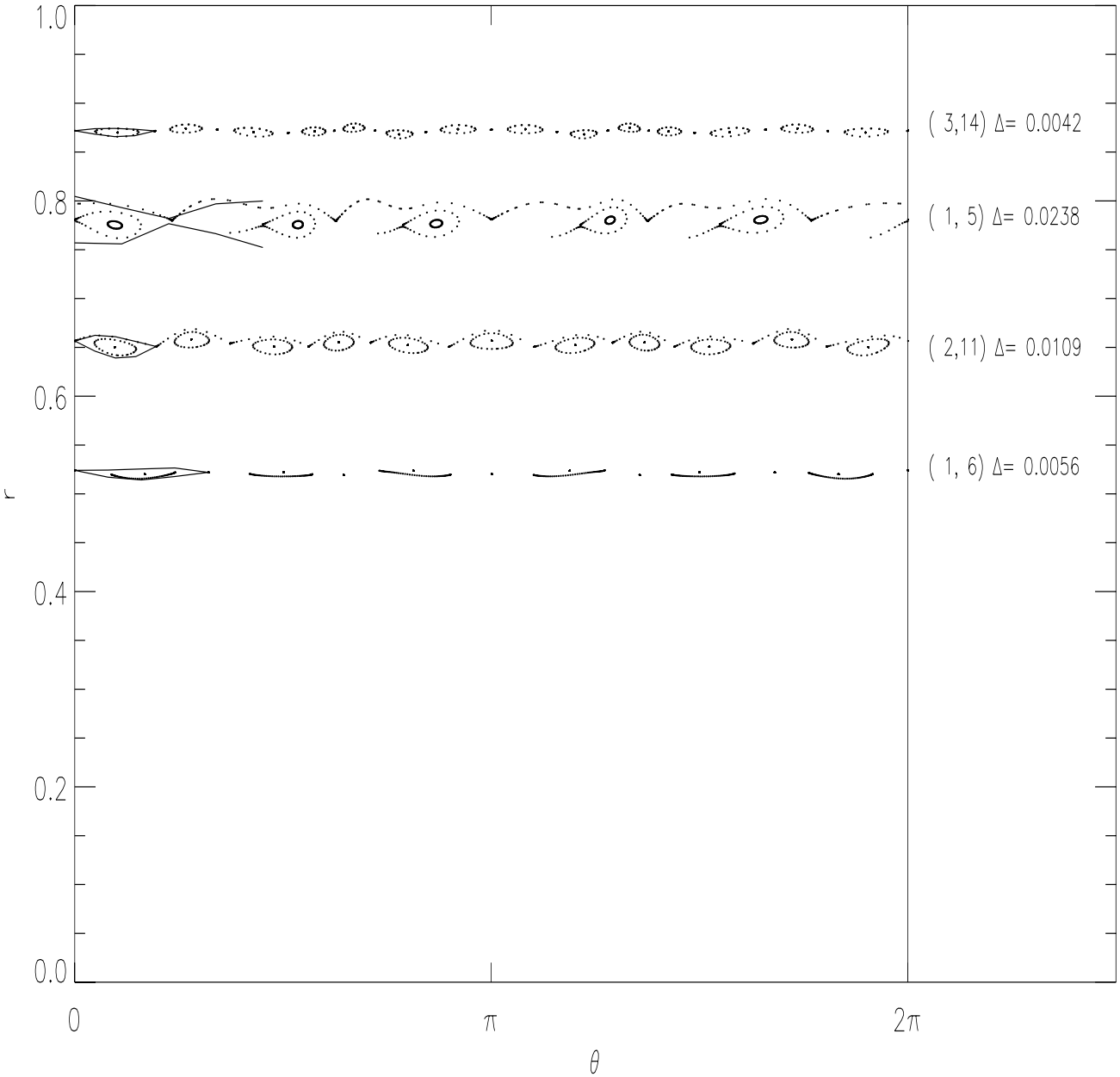

- The $(1,5)$ is reduced, but again the $(2,10)$ is showing. The $(1,6)$ is reduced.

Summary

- Results thus far indicate that it is possible to control the island size using boundary perturbations. Typical boundary perturbations are about one millimeter.

Future work

- Develop algorithm focusing on flexibility and robustness, including implementation of Broyden's method of updating Coupling Matrix.
- Consider more boundary perturbations and higher order islands, in particular the $(2, 10)$.
- Implement free boundary PIES calculations.
- Consider manipulating island phase.
- Extract information regarding the sensitivity of island formation on external fields – design of trim coils.
- Understand underlying driving mechanisms of island formation.

References

[1] R.L. Dewar, S.R. Hudson, and P. Price. Almost invariant manifolds for divergence free fields. *Phys.Lett.A*, 194:49, 1994.

[2] S.R. Hudson and R.L. Dewar. Construction of an integrable case close to any non-integrable toroidal magnetic field. *Phys.Lett.A*, 247:246, 1998.